Available online at www.sciencedirect.com

ScienceDirect

Geochimica et Cosmochimica Acta 315 (2021) 317–332

Geochimica et Cosmochimica Acta

www.elsevier.com/locate/gca

Constraints on coccolithophores under ocean acidification obtained from boron and carbon geochemical approaches

Yi-Wei Liu [a,b,*], Sebastian D Rokitta [c], Björn Rost [c,d], Robert A. Eagle [b,e,f,*]

[a] *Institute of Earth Sciences, Academia Sinica, 128, Sec. 2, Academia Road, Nangang, Taipei 11529, Taiwan*
[b] *Université de Brest, UBO, CNRS, IRD, Ifremer, Institut Universitaire Européen de la Mer, LEMAR, Rue Dumont d'Urville, 29280 Plouzané, France*
[c] *Alfred Wegener Institute - Helmholtz-Centre for Polar- and Marine Research, Am Handelshafen 12, 27570 Bremerhaven, Germany*
[d] *FB Biology/Chemistry, University of Bremen, Leobener Strasse, 28359 Bremen, Germany*
[e] *Institute of the Environment and Sustainability, University of California – Los Angeles, La Kretz Hall, 619 Charles E. Young Dr. E #300, Los Angeles CA90024, USA*
[f] *Atmospheric and Oceanic Sciences Department, University of California –Los Angeles, Math Sciences Building, 520 Portola Plaza, Los Angeles, CA 90095, USA*

Received 21 September 2020; accepted in revised form 20 September 2021; Available online 25 September 2021

Abstract

Ocean acidification (OA) appears to have diverse impacts on calcareous coccolithophores, but the cellular processes underlying these responses are not well understood. Here we use stable boron and carbon isotopes, B/Ca ratios, as well as inorganic and organic carbon production rates to investigate the carbon utilization and the internal pH regulation at the site of calcification in *Emiliania huxleyi*, *Calcidiscus leptoporus* and *Pleurochrysis carterae* cultured over a wide pCO_2 range (180–1000 µatm). Despite large variability, the geochemistry data indicate species-specific modes of pH control and differences in the utilization of inorganic carbon. Boron isotope data suggest that all three species generally upregulate the pH of the calcification fluid (pH_{CF}) compared to surrounding seawater, which coincides with relatively constant growth rates and cellular ratios of inorganic to organic carbon. Furthermore, species exhibit different strategies in regulating their pH_{CF}, i.e., two species maintain homeostasis ($pH_{CF} = \sim 8.7$), while one species shows a constant offset to the surrounding seawater ($\Delta pH = \sim 0.6$ units) over the entire tested pCO_2 range. In addition to these different strategies, carbon isotope data suggests that high plasticity in the utilization of dissolved inorganic carbon might be an explanation for species-specific differences in coccolithophore responses to OA.

Keywords: Ocean acidification; Coccolithophores; Carbon isotopes; Boron isotopes

1. INTRODUCTION

Coccolithophores are calcifying microalgae and are among the most important primary producers in the ocean (Eikrem et al., 2016). They utilize dissolved inorganic carbon (DIC) for both photosynthesis and calcification, and play an important role in regulating carbonate chemistry

* Corresponding authors at: Institute of Earth Sciences, Academia Sinica, 128, Sec. 2, Academia Road, Nangang, Taipei 11529, Taiwan (Y.-W. Liu). Institute of the Environment and Sustainability, University of California – Los Angeles, La Kretz Hall, 619 Charles E. Young Dr. E #300, Los Angeles CA90024, USA (R.A. Eagle).

E-mail addresses: liuyiwei@earth.sinica.edu.tw (Y.-W. Liu), robeagle@g.ucla.edu (R.A. Eagle).

https://doi.org/10.1016/j.gca.2021.09.025
0016-7037/

as well as mediating the flux of carbon dioxide (CO_2) from the atmosphere into the deeper ocean through the biological carbon pump (Rost and Riebesell, 2004). Experiments have shown that the particulate inorganic and organic carbon (PIC, POC) production of coccolithophores, as well as their responses to ocean acidification (OA), vary among species, and even among strains within a species (Langer et al., 2006; Langer et al., 2009; Meyer and Riebesell, 2015).

Emiliania huxleyi is the most abundant coccolithophore in surface waters, and culture studies show that also *E. huxleyi* has highly variable and strain-specific responses in experimentally manipulated OA scenarios (Hoppe et al., 2011; Iglesias-Rodriguez et al., 2008; Langer et al., 2009; Riebesell et al., 2000). Recent studies suggest that this species will shift the relative uptake of inorganic carbon from HCO_3^- towards CO_2 under low pH conditions, and that seawater $[H^+]$ is the primary driver for these OA responses (Kottmeier et al., 2014; Kottmeier et al., 2016b). However, how this species controls the pH and carbonate chemistry in the calcification fluid (pH_{CF}; DIC_{CF}) is still largely unknown.

Calcidiscus leptoporus is a cosmopolitan species thriving in tropical to subtropical oligotrophic warm-water masses. Typical coccolith and coccosphere sizes of *C. leptoporus* range from 3 to 11 μm and 5 to 20 μm, respectively (Geisen et al., 2002; Knappertsbusch et al., 1997), which is significantly larger than *E. huxleyi*. Its coccoliths can be dominant in sediments due to their comparably high dissolution resistance (Boeckel and Baumann, 2004; Dittert et al., 1999). The fossil records of *C. leptoporus* can be traced back to 23 Ma ago (Geisen et al., 2004; Knappertsbusch, 2000). In contrast to *E. huxleyi*, recent culture studies suggest that the calcification process of *C. leptoporus* is not negatively affected by OA (Fiorini et al., 2011; Langer et al., 2006).

Pleurochrysis (also known as *Chrysotila*) *carterae* is a motile coccolithophore species that is widely distributed along the temperate coasts of Europe (van den Hoek et al., 1995). Different from the well-studied coccolithophore species *E. huxleyi*, the considerably larger *P. carterae* has a relatively high content of particulate organic carbon (POC) compared to the calcite, with typical PIC:POC ratios lower than 0.5 (e.g., Casareto et al. (2009); White et al. (2018)). In addition, special polysaccharides form organic nucleation matrices and assist in calcification, which has been recognized as a distinct biomineralization pathway in this species (Marsh, 2003). The organic matrix is occluded in the calcite during the precipitation process, causing a high organic content of the calcite composite material formed by *P. carterae* (Hood et al., 2016; Moheimani and Borowitzka, 2011). These differences suggest that *P. carterae* allocates DIC to the calcification vesicle in a different way than the aforementioned species, and also point towards differences in its internal carbonate chemistry regulation.

The chemical composition of coccolith calcite can be used as a tracer for physiological processes in the organisms and for environmental conditions during calcification. Previous studies have utilized ^{13}C in both, organic components and coccolith calcite to infer carbon utilization in the organism (Hermoso, 2015; Hermoso et al., 2016; McClelland et al., 2017; Rickaby et al., 2010; Rost et al., 2002). Similar to other phytoplankton, the extent to which stable carbon is fractionated can be attributed to fluxes of DIC into the cell, leakage of carbon from the chloroplast or the cell, the location and activity of the enzyme carbonic anhydrase (CA) and/or the rate of calcification (Eichner et al., 2015; Hoins et al., 2016; Hoins et al., 2015; McClelland et al., 2017). Although CA may not always play a role with regard to fractionation (Hoins et al., 2016; McClelland et al., 2017), Eichner et al. (2015) has shown that CA-like activities have the potential to modify isotopic values of carbon species and thus overall fractionation. As proposed models describe the observed fractionation only adequately for certain species or pCO_2 ranges (e.g., Hoins et al. (2016); Hoins et al. (2015); McClelland et al. (2017)), we apparently still lack sufficient understanding of the processes controlling the isotopic fractionation, which is especially true for coccolithophore species of different origin and ecology. Thus, more laboratory and field data are needed to better constrain the underlying processes and to improve interpretations of the carbon fractionation data from experiments or geological records.

In addition, boron geochemistry can be used to constrain the pH_{CF} and other carbonate system parameters. This approach has been widely used in corals and other calcifiers (Liu et al., 2020; McCulloch et al., 2018), but is less developed in coccolithophores, partly due to the difficulty of measuring the low boron contents of coccoliths. The few studies available on coccolithophores have shown that the B/Ca ratio and its pH-dependency can vary among species and strains, but it was postulated that a combination of B/Ca and boron isotope measurements could be used to disentangle how coccolithophores regulate their internal carbonate chemistry (Stoll et al., 2012). A follow-up study suggested, however, that coccolith $\delta^{11}B$ of *E. huxleyi* is insensitive to seawater pH changes and might be affected by the nutrient concentration in the culture media (Henehan, 2015). More recently, Liu et al. (2018) showed that the widespread coastal coccolithophore *Ochrosphaera neapolitana* maintains a homeostatic pH at the calcification site. Whether the pH homeostasis and the level of pH regulation is a species-specific characteristic thus remains unresolved.

To address these open questions, we here use a combined $\delta^{13}C$ and boron geochemistry approach to study carbon utilization and pH regulation in three coccolithophore species (*E. huxleyi, C. leptoporus* and *P. carterae*) that are common members of phytoplankton assemblages but originate from different lineages with contrasting ecologies. These species were acclimated to a range of pCO_2/pH reflecting not only oceanic carbon chemistry from glacial to interglacial times, but also the conditions projected for the year 2100 (IPCC, 2013). We assess their (1) photosynthetic and calcification responses to CO_2-induced OA using their PIC/POC ratio, (2) utilization of carbon species in calcification and photosynthesis using stable carbon isotopes, and (3) the ability to regulate the carbonate chemistry of the calcifying fluid using boron isotopes and B/Ca ratios as a pH proxy.

2. MATERIALS AND METHODS

2.1. Culture experiment

Three strains of different coccolithophore species *Emiliania huxleyi* (RCC 1216, a heavily calcified 'R' morphotype), *Calcidiscus leptoporus* (RCC 1129) and *Pleurochrysis carterae* (PCC156) were grown as dilute-batch cultures at 17 ± 1 °C in 0.2 µm (PES) filtered North-Sea seawater medium (Salinity ~ 33 PSU) that was enriched with nutrients (100 µM NO_3^-; 6 µM PO_4^{3-}) as well as vitamins and trace metals according to the F/2 recipe by Guillard and Ryther (1962). The three species were selected because of their generally different cell sizes, calcification levels and responses to OA (Meyer and Riebesell, 2015; Moheimani and Borowitzka, 2011). The algal cultures were grown under a 16:8h light:dark cycle with an irradiance of 150 ± 15 µmol photons m^{-2} s^{-1} (OSRAM daylight lamps Biolux 965) that was measured with a 4π-sensor (US-SQS/L, ULM 500; Walz, Effeltrich, Germany). Cultivation vessels were 2.5 L polycarbonate bottles (Nalgene; New York, USA) on automated roller tables to maintain suspension of cells. Before inoculating cells into the experiments, cells were pre-acclimated to experimental conditions and the respective pCO_2 for at least 10 division cycles. Throughout the experiment, we refrained from using glass-made material to avoid a bleeding of boron compounds into the water that would interfere with analytical procedures. To adjust pCO_2, culture media were pre-aerated with humidified, 0.2 µm filtered air with adjusted pCO_2 (180, 380, 750, 1000 µatm) that were created using a gas-flow controller (CGM2000; MCZ Umwelttechnik, Bad Nauheim, Germany), which mixed pure CO_2 (AirLiquide, Düsseldorf, Germany) into CO_2-free air (CO_2-stripper; Domnick-Hunter, Willich, Germany). Target pCO_2 values were monitored regularly with a non-dispersive infrared analyzer (LI6252, Li-Cor) and via the measured wet-chemical parameters.

Algae samplings were done 6–10 hours after the beginning of the light period, i.e., at midday with mean algal densities of 52000 mL^{-1} (*E. huxleyi*), 4300 mL^{-1} (*C. leptoporus*) and 4900 mL^{-1} (*P. carterae*). The cell densities were kept intentionally low to prevent large drifts in carbonate chemistry while obtaining sufficient materials for elemental and isotopic analyses. Cell densities differed slightly between biological replicates at the time of sampling because of small deviations in the inoculation and/or growth rates. In few instances, cell densities exceeded target values leading to larger shifts in carbonate chemistry. The carbonate systems in the cultures were determined in the beginning and the end of the cultivation: The seawater pH (pH_{SW}; in NBS scale) was assessed daily or every other day with a regularly calibrated handheld device (826 pH mobile device with an Aquatrode Plus; Metrohm, Filderstadt, Germany) and corrected for daily offsets by including measurements of a TRIS reference buffer (Dickson et al., 2007). The instrumental uncertainty given by the manufacturer is ± 0.001 pH unit. The pH reproducibility of each measurement was typically smaller than 0.003 pH unit (n = 3). The variation between the three biological replicates was typically smaller than 0.03 pH units. The pH_{SW} value reported in the figures and supplemental information is the average of the initial and the end pH measurements, and the uncertainty of the pH reported (1 SD) denotes the variation of the pH in the cultivation vessel during the experiment instead of the uncertainty of the pH measurements. DIC was assessed from sterile-filtered media with the colorimetric method developed by Stoll et al. (2001), using a QuAAtro autoanalyzer (Seal Analytical, Norderstedt, Germany). For completeness, also TA was assessed from linear Gran titration plots (Dickson, 1981), which were produced using an autosampler-coupled burette system (TitroLine alpha plus, Schott, Mainz, Germany). Both, DIC and TA were corrected for daily offsets by including certified reference materials (CRM) obtained from A. Dickson (Scripps Institution of Oceanography). The complete carbonate systems were calculated based on pH_{SW} and dissolved inorganic carbon (DIC) using the CO2SYS package (Pierrot et al., 2006), as well as temperature, salinity and pressure (Hoppe et al., 2012). For all calculations, the concentrations of phosphate and silicate were assumed to be 6 and 1 µM, respectively. Equilibrium constants for carbonic acid were adapted from Dickson and Millero (1987), who refitted the data obtained by Mehrbach et al. (1973). For sulfuric acid, the dissociation constants described by -Dickson, 1990 were used and total boron concentration reported by Lee et al. (2010) was used.

Based on our DIC data, we have shown that DIC drawdown was <152 µmol kg^{-1}, which translate into a theoretical nitrate and phosphate drawdown of 24 and 1.5 µM, respectively. Thus, the supplied nutrient levels of 100 µM nitrate and 6.6 µM phosphate must have remained sufficiently high, ruling out nutrient limitation.

2.2. Growth, elemental and isotopic analysis

Algal culture growth was monitored by daily cell counts with a particle counter (Multi-Sizer III, Beckman-Coulter, Fullerton, CA, USA), and specific growth rates (μ) were assessed from daily increments using the equation $\mu = (\ln(c_1) - \ln(c_0))\ \Delta t^{-1}$, where c_0 and c_1 are the cell concentrations at two time points and Δt is the time interval in days.

For the determination of total particulate carbon (TPC), particulate organic carbon (POC), as well as the carbon isotopic signatures ($\delta^{13}C$), cultures were gently vacuum-filtered (−200 mbar relative to the atmosphere) onto pre-combusted (3 h at 500 °C) GF/F filters (Whatman, Maidstone, UK), which were dried at 50 °C and analyzed on an ANCA SL 20–20 stable isotope mass spectrometer (SerCon; Crewe, UK). Before the quantification of POC, the respective filters were soaked with 0.2 M HCl and dried again, to remove calcite. Particulate inorganic carbon (PIC) was assessed as the replicate-specific difference between TPC and POC. By multiplying elemental quotas with specific growth rates, the respective production rates could be assessed (Rokitta and Rost, 2012).

For the assessment of the boron isotopic signatures, trace elemental ratios and carbon isotopic signatures in coccolith calcite, cell cultures were concentrated by gentle filtration on polycarbonate membrane filters (47 mm

diameter, 1 μm pore size; Whatman® Nuclepore™, GE Healthcare, UK) and concentrated algal suspension was centrifuged (~10 min at 13.000*g*) to pellet cells. The supernatant was then discarded and the cell pellet was dried at 50 °C in an oven. Dry samples were packed and transferred to a clean lab for further cleaning and chemical treatments.

Before chemical analysis, the dry samples were first rinsed with Milli-Q water (MQ; 18 MΩ·cm) three times to remove remaining salt precipitates on the cells. About 100 μg of sample split was then prepared for stable isotope analysis. The $\delta^{13}C$ of coccolith calcite was analyzed on a Finnigan MAT Kiel IV preparation device coupled directly to the inlet of a Finnigan MAT 253 triple collector isotope ratio mass spectrometer in the stable isotope lab in the Global Change Research Center, National Taiwan University, Taiwan. The reproducibility of the reference standard NBS-19 and an in-house carbonate standard MAB were better than ±0.09‰ (2 SD, $n = 4$) and ±0.15‰ (2 SD, $n = 16$), respectively.

Stable carbon isotopes of dissolved inorganic carbon ($\delta^{13}C_{DIC}$) were measured via a Finnigan MAT Delta Plus XL mass spectrometer in continuous flow mode connected to a Gas Bench with a CombiPAL autosampler in the Stable Isotope Lab in the Department of Geological and Atmospheric Sciences, Iowa State University, USA. Reference standards (NBS-18, NBS-19) were used for isotopic corrections, and to convert data to be relative to the Vienna PeeDee Belemnite (VPDB) value. At least one reference standard was used for every five samples. The combined uncertainty of analytical reproducibility and average correction factor for $\delta^{13}C_{DIC}$ is ± 0.09‰ (VPDB).

Boron isotopic composition in coccolith samples was measured following the method from Liu et al. (2013, 2015). Micro-sublimation and total evaporation negative ion thermal ionization mass spectrometry (TE-NTIMS) techniques were applied. The methods were used due to limited amount of boron available and to avoid extra contamination introduced during purification. In brief, less than 50 μL of standard or sample solution with [B] = ~750 ppb was loaded onto a cap of conical bottom Savillex PFA vial for 15 hours of sublimation. After purification, 2 μL of 30% ultrapure H_2O_2 was added to remove additional organic materials and eliminate potential interferences of CN^- when running isotope analysis. 1 μl of standard or sample was then loaded onto a refined Re-filament after 1 μL of boron free seawater (BFSW) was loaded. Boron isotopes were analyzed using a Thermo Fisher Triton multicollector thermal ionization mass spectrometer operating in negative ion mode (NTIMS) at the Institute of Earth Sciences, Academia Sinica, Taiwan. The same amount of carbonate standard JCp-1 was processed using the same protocols as the coccolith samples to monitor the robustness of the method. Boron isotopic composition in seawater and coccolith samples were reported as $\delta^{11}B$, where

$$\delta^{11}B = \left[\frac{(^{11}B/^{10}B)_{sample}}{(^{11}B/^{10}B)_{SRM\ 951a}} - 1\right] \times 1000\ (‰) \quad (1)$$

with $^{11}B/^{10}B$ for boric acid standard SRM 951a was 4.034 5 ± 0.0084‰ (2 SD, $n = 24$). Boron isotopic composition in seawater medium was analyzed on a Finnigan Neptune multicollector-inductively coupled plasma mass spectrometer (MC-ICPMS) at IFREMER, France. The reproducibility of $\delta^{11}B$ determinations in seawater analyzed on MC-ICPMS was ±0.58‰ (2 SD, $n = 12$) and the reproducibility of $\delta^{11}B$ determinations in international coral standard JCp-1 analyzed on NTIMS were ±1.9‰ (2 SD, $n = 23$) and 1.66‰ (2 SD, $n = 38$), before and after replacing an ion source, respectively.

There are two dominant dissolved boron species in seawater, boric acid and the borate ion. The relative proportion of these two species is pH-dependent and the reaction can be described by the following reaction equation:

$$B(OH)_3 + H_2O \rightleftharpoons B(OH)_4^- + H^+ \quad (2)$$

The isotope exchange between two species follows the reaction below:

$$^{10}B(OH)_3 + {}^{11}B(OH)_4^- \rightleftharpoons {}^{11}B(OH)_3 + {}^{10}B(OH)_4^- \quad (3)$$

where ^{11}B is enriched in boric acid compared to the borate ion. The boron isotopic signature can therefore be determined after combining the reactions above, with a fractionation factor (α) between the two species of 1.0272 (Klochko et al., 2006). Although more recent studies have derived a range of fractionation factors based on theoretical calculations (1.026–1.028 (Nir et al., 2015; Rustad et al., 2010)), the uncertainties of these are larger than the value obtained by Klochko et al. (2006). Therefore, $\alpha = 1.0272$ is widely used by the community and also applied in the present study.

It has been hypothesized and also observed that marine carbonates primarily incorporate $B(OH)_4^-$ into the carbonate structure during their shell growth, and therefore seawater pH not only dictates the amount of $B(OH)_4^-$ in seawater but also the isotopic composition of boron in marine carbonates. In this case, the seawater pH can be derived based on the equation:

$$pH = pK_b - \log\left(-\frac{\delta^{11}B_{sw} - \delta^{11}B_{carbonate}}{\delta^{11}B_{sw} - \alpha\delta^{11}B_{carbonate} - 1000(\alpha - 1)}\right) \quad (4)$$

Marine calcifiers precipitate their calcium carbonate skeletons/shells from an enclosed or semi-enclosed compartment, where the pH can be regulated and thus potentially differ from the ambient bulk seawater. Instead of directly reflecting ambient seawater pH, the boron isotopic signature is therefore dictated by the pH of the calcification site fluid pH, and can be calculated based on the adjusted equation:

$$pH_{CF} = pK_b - \log\left(-\frac{\delta^{11}B_{CF} - \delta^{11}B_{carbonate}}{\delta^{11}B_{CF} - \alpha\delta^{11}B_{carbonate} - 1000(\alpha - 1)}\right) \quad (5)$$

It has been proposed that boric acid is the only dissolved boron species that permeates membranes (Stoll et al., 2012), based on findings of nearly identical boron concentrations in external and internal medium of plant cells (Brown and

Hu, 1993; Seresinhe and Oertli, 1991), suggesting a passive transport of boron. Alternatively, although energetically costly, it has been demonstrated that active transport of borate ion via transporters BOR or NIP is possible during boron deficiency (Takano et al., 2005; Takano et al., 2002; Tanaka and Fujiwara, 2008). Because boron concentration in seawater is ~4-fold higher than that in soil, Stoll et al. (2012) therefore suggest passive diffusion of non-charged boric acid as the principle boron uptake mechanism in coccolithophores. Because of the high permeability of lipid bilayers to boric acid, the boron concentration is thought to reach close-to-equilibrium levels across cell membranes (Dordas and Brown, 2000). However, boron isotopic composition of the coastal coccolithophore species *Ochrosphaera neapolitana* shows lower values than predicted based on the model that assumes that boric acid exclusively enters the coccolith vesicle (Liu et al., 2018). Whether boric acid is the only species that can be transported across coccolithophore cell membrane and vesicle is still under investigation. Therefore, here we test both scenarios, in which either the boron isotopic signature is the same in the calcifying fluid and the seawater ($\delta^{11}B_{CF} = \delta^{11}B_{SW}$), or the boron isotopic signature of the calcifying fluid carries the isotopic signal of boric acid in the seawater ($\delta^{11}B_{CF} = \delta^{11}B_{seawater\ boric\ acid}$).

The coccolith B/Ca analysis were conducted on a high resolution ICP-MS ELEMENT XR at the Institute of Earth Sciences, Academia Sinica. The reproducibility of B/Ca is generally better than ±2% (2 RSD, relative standard deviation) for B/Ca values greater than 200 μmol/mol, and still ±12% (2 RSD) for B/Ca values smaller than 25 μmol/mol. To avoid interference of B from the organic matrix, an improved oxidation and cleaning protocol has been applied. The validation of the stepwise cleaning protocol is detailed in the supplementary materials (S1). In brief, samples were treated overnight with 15% H_2O_2 (pH adjusted to >8 by adding NaOH) before dissolving the coccolith carbonate. Although it has been suggested that a combined reductive and oxidation cleaning protocols are more efficient to remove organic matrix that bonded with coccoliths (Blanco-Ameijeiras et al., 2012; Henehan, 2015), it is also known that reductive cleaning protocols can result in substantial loss of sample materials. As complex cleaning procedures could risk introducing higher blanks, we applied a cleaning protocol using a single but stronger oxidation reaction. Based on tests with different concentrations of H_2O_2 (Fig. S1), 15% solutions were applied to our samples. The calcium running concentration of the standards and solution was 2 mM.

To further evaluate the potential interferences of organic remnants, we also monitored other trace elemental ratios. Particularly, Fe/Ca and P/Ca ratios of coccoliths have been used to assess the effectiveness of cleaning coccolith samples (Blanco-Ameijeiras et al., 2012). Although we do not have P/Ca results available, we do have Fe/Ca ratios monitored for both, samples of the original experiment as well as from the additional cleaning test, allowing us to further assess the cleanness of the sample.

Our results suggest that high Fe/Ca ratios do not significantly bias B/Ca ratios if the ratios are lower than 1000 μmol/mol ($df = 8$, $P = 0.08$, CI = 95%; Fig. S3). This was because the B/Ca values were nearly identical based on the current analytical resolution, which is 12% for 25 μmol/mol of B/Ca. This Fe/Ca level is also below the range of coccolithophore Fe/Ca after applying the optimal cleaning protocol on the cultured *E. huxleyi* and *C. leptoporus* reported in Blanco-Ameijeiras et al. (2012) (Fig. S2(d)). We therefore set 1000 μmol/mol of Fe/Ca as additional filter threshold to re-assess the data set of our pH control experiment. Based on our described screening procedure, we removed one data point from *C. leptoporus* and two data points from *P. carterae*, respectively (Fig. S4). We find that our cleaning methods give B/Ca values that are comparable to those reported for *E. huxleyi* by Diez Fernández et al. (2015) and Henehan (2015) (Fig. S2). In addition, the vast majority of Fe/Ca data fall within the range reported in Blanco-Ameijeiras et al. (2012) for the combined reductive and oxidative cleaning. Thus, we overall conclude that our B/Ca data is comparable to that reported in previous publications (Blanco-Ameijeiras et al., 2012; Diez Fernández et al., 2015; Henehan, 2015), and thereby we have confidence in our boron isotope data.

In addition to the aforementioned analysis, about 1 mL of culture was filtered onto 25 mm polycarbonate filters (Whatman) and sputtered for scanning electron microscopy (SEM) analysis (Figs. S5–S7). The overall sample processing protocols are illustrated in Fig. S8.

2.3. Statistical evaluation

All linear regressions were calculated with least squares method to check for statistically significant trends with respect to seawater pH treatments. Trends were deemed significant when P values were ≤ 0.05. Propagated errors of boron-inferred pH_{CF} were calculated via Monte Carlo simulations.

3. RESULTS

3.1. Growth rates and PIC/POC variations

Coccolithophore specific growth rates, PIC/POC ratios, POC and PIC quotas as well as POC and PIC productions are plotted against culture seawater pH in Fig. 1. There is no statistically significant trend in specific growth rates, PIC/POC ratios, or carbon production rates in any of the tested species. Average cell growth rates of *E. huxleyi*, *C. leptoporus*, and *P. carterae* are 0.83, 0.36, and 0.83 d^{-1}, respectively (Fig. 1(a)). The specific growth rates of *P. carterae* increased during the last two days before harvesting, resulting in large standard deviations for the growth rate estimates in this species. Nevertheless, a positive correlation is found between the PIC quota of *E. huxleyi* and seawater pH ($R^2 = 0.40$, $P < 0.03$), albeit weak. The PIC/POC ratios of the three coccolithophore species do not show consistent responses to pH_{SW} (Fig. 1(b)), but correlate with diverse

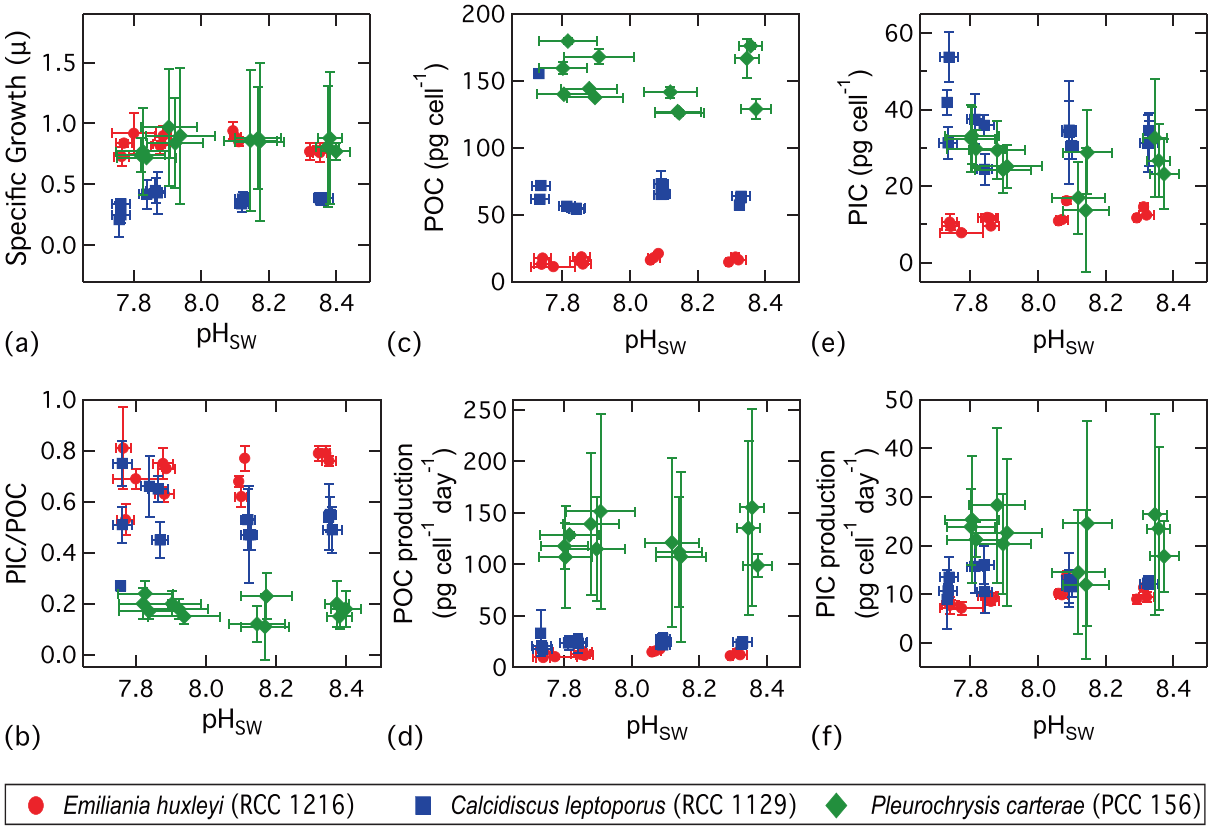

Fig. 1. The growth, PIC/POC, POC quota, POC production, PIC quota, and PIC production as a function of pH_{SW}. The (a) specific growth (μ), (b) PIC/POC ratios, (c) POC quota (pg cell^{-1}), (d) POC production (pg cell^{-1} day^{-1}), (e) PIC quota (pg cell^{-1}), and (f) PIC production (pg cell^{-1} day^{-1}) of coccolithophore species *E. huxleyi*, *C. leptoporus*, and *P. carterae* are shown in red circles, blue squares, and green diamonds, respectively. The error bars denote one standard deviation (SD) of the analysis or propagated uncertainty of the calculation.

biological parameters. In *E. huxleyi*, PIC/POC shows a larger variation in the low pH treatments. The PIC/POC ratio in *C. leptoporus* is negatively correlated to POC quota ($R^2 = 0.42$, $P = 0.02$), but is positively correlated to the PIC production rate ($R^2 = 0.68$, $P < 0.01$). The PIC/POC ratio in *P. carterae* is positively correlated to the PIC quota ($R^2 = 0.72$, $P < 0.01$).

The PIC/POC ratios of the three species show distinctively different values, with the values of *E. huxleyi* being the highest, followed by *C. leptoporus*, and the PIC/POC ratios of *P. carterae* being the lowest. Note that the PIC/POC ratios of *C. leptoporus*, which is thought to be heavily calcified, are lower than expected based on literature values (Diner et al., 2015; Fiorini et al., 2011; Hermoso et al., 2014; Langer et al., 2006). By checking the SEM images (see Supplementary material S2, and Figs. S5–S7), we found a major presence of holococcoliths instead of the typical heterococcoliths of *C. leptoporus* that are more heavily calcified, which explains the relatively low PIC/POC values in our study. Although variations exist within the growth rates and PIC/POC ratios in each treatment of the experiment, the results demonstrate that the selected species cover different ranges of growth rates and PIC/POC ratios. Moreover, PIC/POC ratios do not systematically follow a certain response pattern that holds true across these taxonomically different coccolithophores.

3.2. Carbon and boron isotope results

The isotopic composition of the POC and PIC were normalized to the carbon isotopic composition of the culture seawater DIC in order to remove signals derived from differences in the inorganic carbon source (e.g., from fossil CO_2 introduced by bubbling). Therefore, the carbon isotope results are reported with a Δ notation. Here, we define that $\Delta^{13}C_{POC} = \delta^{13}C_{POC} - \delta^{13}C_{DIC}$, and $\Delta^{13}C_{PIC} = \delta^{13}C_{PIC} - \delta^{13}C_{DIC}$. The $\Delta^{13}C_{POC}$ and $\Delta^{13}C_{PIC}$ values of the three species range between $-30‰$ and $-10‰$, and between $-2.5‰$ and $2‰$, respectively (Fig. 2). Within each species, we found similar pH-dependencies between the $\Delta^{13}C_{POC}$ and $\Delta^{13}C_{PIC}$. In *E. huxleyi,* there is no trend between seawater pH and carbon isotopes in either $\Delta^{13}C_{POC}$ and $\Delta^{13}C_{PIC}$. In *C. leptoporus*, $\Delta^{13}C_{POC}$ and $\Delta^{13}C_{PIC}$ are threshold negatively and negatively correlated to the seawater pH respectively ($R^2 = 0.67$, $P < 0.01$ and $R^2 = 0.98$, $P < 0.01$). In *P. carterae,* $\Delta^{13}C_{POC}$ and $\Delta^{13}C_{PIC}$ values show positive correlation with the seawater pH ($R^2 = 0.74$, $P < 0.01$ and $R^2 = 0.33$, $P = 0.06$, respectively).

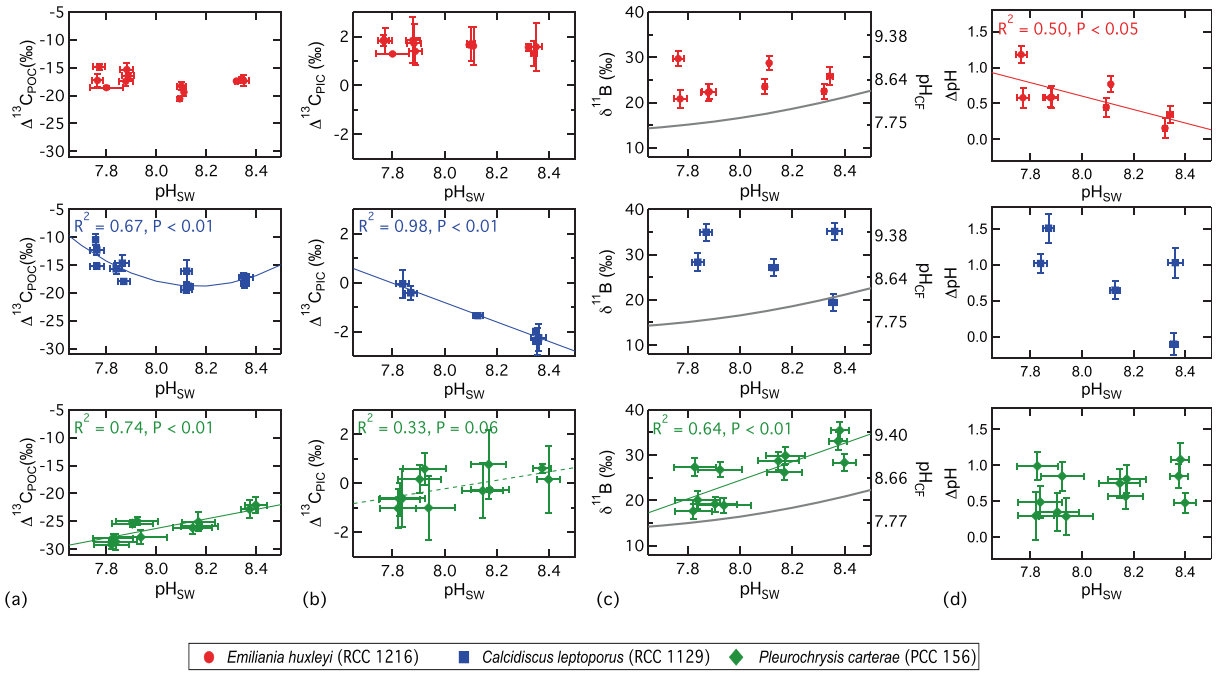

Fig. 2. Stable carbon and boron isotope results as a function of seawater pH (a) and (b) show the carbon isotopic composition of particulate organic and inorganic carbon, respectively. (c) and (d) are boron isotopic compositions and the pH offsets between calcification site fluid and the ambient seawater, respectively. *E. huxleyi*, *C. leptoporus*, and *P. carterae* are shown in red circles, blue squares, and green diamonds, respectively. The error bars of carbon and boron isotopes and calculated pH offsets represent 2 SD of the results, while the horizontal error bars show the 1 SD of the pH values. Note that the 2 SD of boron isotopes here were obtained from the long-term reproducibility of international coral standard JCp-1 because the coccolith material were limited for replications for most of the sample. Gray lines are theoretical borate fractionation curves ($\alpha = 1.0272$; Klochko et al., 2006). Solid red, blue and green lines denote statistically significant linear/nonlinear trends of the data set (Tables S1–S5). Dotted lines indicate weaker significance in linear trends ($0.05 < p < 0.1$).

Boron isotopic compositions range between 15‰ and 35‰ (Fig. 2(c)). The $\delta^{11}B$ values of *E. huxleyi* show little change across the different pH treatments, while the $\delta^{11}B$ values of *C. leptoporus* generally display larger variability even within the same treatments. For *P. carterae,* we found that $\delta^{11}B$ values were positively correlated to seawater pH ($R^2 = 0.64$, $P < 0.01$). These boron isotopic data can be translated to a pH_{CF} range between 7.8 and 9.5 (Fig. 2(c), and Fig. 3(a)), based on the assumption that $\delta^{11}B_{CF} = \delta^{11}B_{SW}$ and that only borate ions are incorporated into the calcite structure. To further evaluate the abilities of coccolithophores to regulate the pH_{CF}, we calculate the ΔpH values and plot them against pH_{SW} (Fig. 2(d)). By doing so, it becomes clear that *E. huxleyi* and *C. leptoporus* elevate their pH_{CF} by about 1.0 pH unit at pH_{SW} 7.8, whereas they only elevated their pH_{CF} by less than 0.5 pH units at $pH_{SW} > 8.3$. In contrast, *P. carterae* shows no trend in ΔpH, i.e., they elevate the pH_{CF} by about 0.6 units independent of the external pH_{SW}. Note that the assumption of the canonical boron systematics applied here might not hold true for all marine organisms. If the alternative hypothesis is used, i.e., that only boric acid is permeable to cell membranes (Stoll et al., 2012), calculations yield slightly lower pH_{CF} values (Fig. 3(b)), resulting in even more pronounced species-specific differences in the relationship between ΔpH and pH_{SW} (Fig. 3(c)). Importantly, both models for interpreting coccolith $\delta^{11}B$ indicate that pH_{CF} levels are all at least about 0.3 pH unit above the ambient pH_{SW}.

3.3. B/Ca

A suite of trace elements was measured, allowing us to report ratios between these trace elements and specifically calcium with the intent to use these ratios as further indicators of biological processes. The complete data can be found in the supplementary materials while here we only focus our analyses on the B/Ca ratio. The cleaning and analytical protocols were optimized on *E. huxleyi* (Fig. S1, 2, and supplementary material S1) and then applied to all species. To further evaluate the cleanness of the sample, we applied an additional quality filter to the dataset, and exclude the results if Fe/Ca ratios are higher than 1000 μmol/mol which we judged to indicate organic and potentially iron oxide contamination (see SI for in depth justification). Generally, B/Ca ratios are different among species. In *E. huxleyi*, the B/Ca ratios are constantly below 25 μmol/mol, in *C. leptoporus,* ratios are close to 100 μmol/mol, but in *P. carterae*, determined ratios are between 14 and 150 μmol/mol (Fig. 4(a)). Regarding the latter, the B/Ca ratios exhibit high variability of about 50 μmol/mol within a treatment, and over 50 μmol/mol between treatments. Overall, there is no significant trend in either of the species against culture seawater pH.

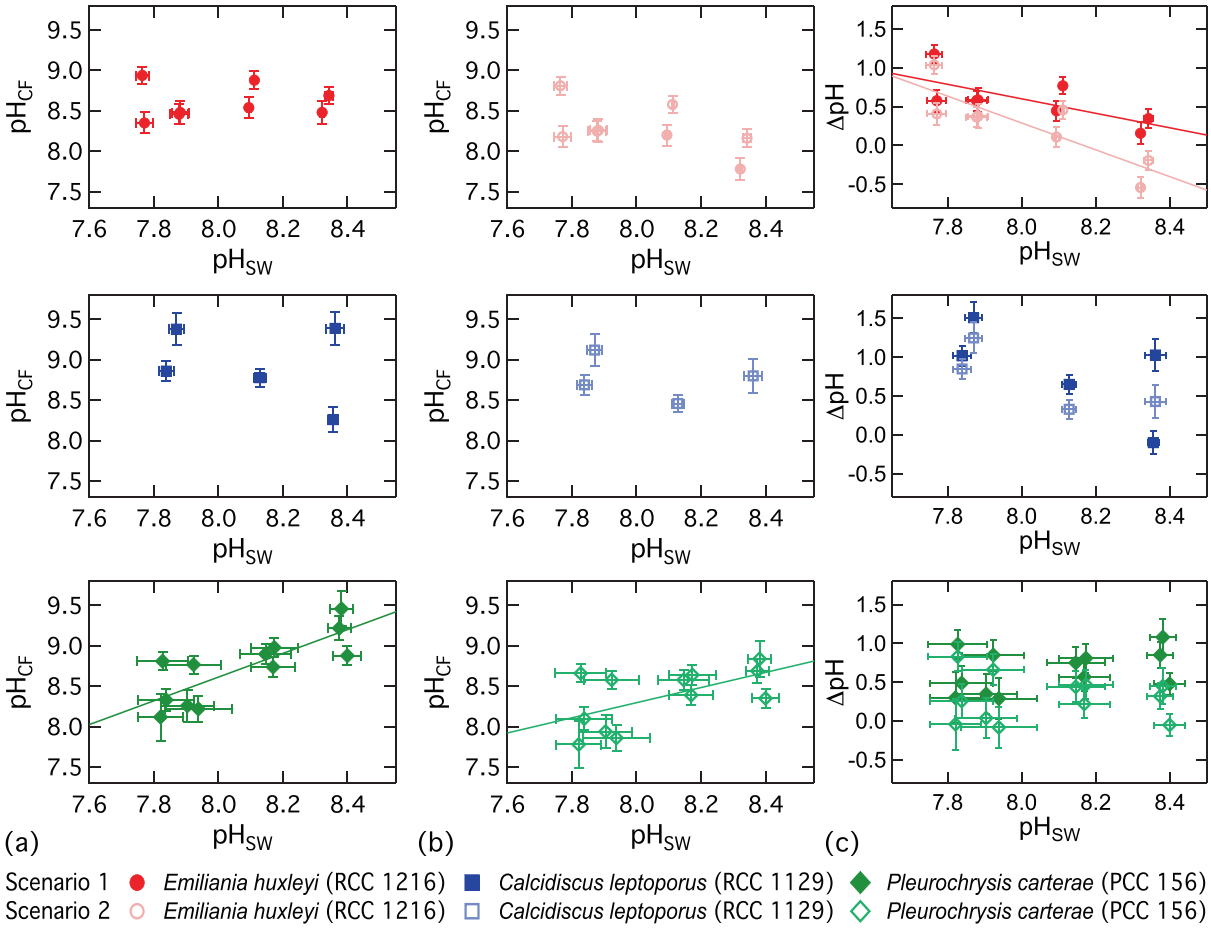

Fig. 3. The $\delta^{11}B$-inferred pH_{CF} values of the three coccolithophore species and their pH offsets to the culture seawater pH. (a) and (b) show the pH_{CF} values that calculated under two different boron transport scenarios. (a) shows the results assuming that both boric acid and the borate ion can be transported through the coccolithophore cell membrane, and the $\delta^{11}B$ value in the calcification site is in isotope equilibrium with the culture seawater $\delta^{11}B$ value. (b) shows the results assuming only boric acid is permeable to the coccolithophore cell membrane, so the total boron concentration and the $\delta^{11}B$ value of the calcification fluid varies depending on the boric acid concentration and its $\delta^{11}B$ value of the culture medium under the control pH conditions. The solid lines show statistically significant linear correlations of the data in the panels.

4. DISCUSSION

4.1. Growth, elemental quotas and production rates

In *E. huxleyi*, the applied pH treatments did not significantly affect growth rates or quotas of POC and PIC (Fig. 1(a, c, e)). Consequently, derived PIC/POC ratios did not show significant trends in response to OA (Fig. 1 (b)). However, the quotas of PIC and POC slightly decreased in more acidic treatments in *E. huxleyi*. This is in line with previous observations for this strain of *E. huxleyi,* especially for the here applied growth-saturating light levels (Kottmeier et al., 2016b; Rokitta and Rost, 2012). Reported PIC production rates showed decreasing or no trend with pH, depending on different culture approaches and conditions (e.g., light regimes) that significantly affect experimental outcomes.

In *C. leptoporus* and *P. carterae*, growth rates were slightly decreased in the lowest pH scenarios, but when considering the whole range of applied pH and the inherent variability of the data, no significant trends in growth rates as well as in quotas and production rates of POC and PIC could be recognized by the applied tests. In contrast to the slightly declining trend in PIC and POC quota observed in *E. huxleyi,* the PIC and POC quota of *C. leptoporus* and *P. carterae* are more resistant to low pH or are even slightly increased under the most acidic condition. The above results suggest that although the PIC/POC ratios of all three species show no clear response to OA, this strain of *E. huxleyi* might still be negatively impacted as both, inorganic and organic production decrease under low seawater pH.

4.2. Carbon isotopic composition and implications for inorganic carbon sources

$\Delta^{13}C_{POC}$ and $\Delta^{13}C_{PIC}$ behave similarly, but show species-specific trends depending on seawater pH (Fig. 2

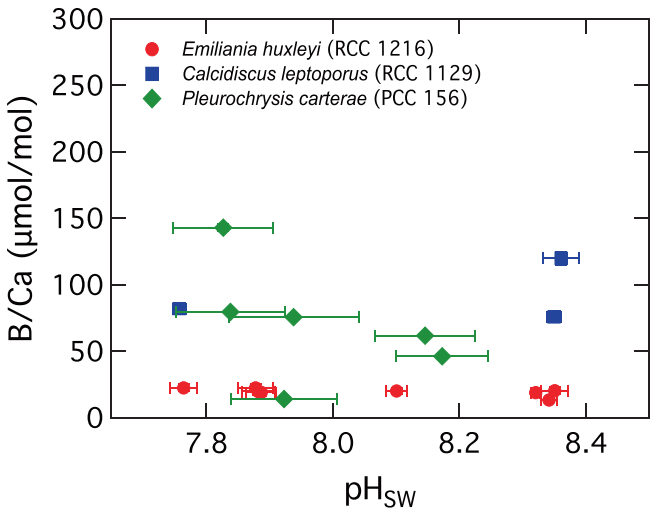

Fig. 4. The B/Ca compositions of coccolithophores as a function of seawater pH (a) The B/Ca of *E. huxleyi*, *C. leptoporus*, and *P. carterae* are shown in red circles, blue squares, and green diamonds, respectively.

(a, b)), being either invariant (as in *E. huxleyi*), decreasing (as in *C. leptoporus*) or increasing (as in *P. carterae*). These differences in trends among species have been proposed to originate mainly from the interplay of species-specific controls on influx of CO_2 vs. HCO_3^-, CO_2 leakage from chloroplasts or the cytosol, as well as Rayleigh fractionation resulting from the interplay of RubisCO fractionation and leakage (McClelland et al., 2017). Disequilibria between CO_2 and HCO_3^- due to changes of vesicle pH or unidirectional "CA-like" processes (Eichner et al., 2015; Wilkes and Pearson, 2019) can also potentially determine how much the intrinsic fractionation of RubisCO can manifest in the isotopic value of POC, and in case of coccolithophores also of PIC (Bolton and Stoll, 2013; Holtz et al., 2017). In the following, we discuss the potential explanations for each species.

Most intuitive is the interpretation of the composition of *P. carterae*: $\Delta^{13}C_{POC}$ values increase with increasing pH (Fig. 2(a, b)), suggesting higher CO_2 usage for photosynthesis under lower pH, which is in line with the current understanding of algal CO_2 concentrating mechanisms (Giordano et al., 2005; Kottmeier et al., 2016b; Reinfelder, 2011). The $\Delta^{13}C_{PIC}$ values are close to zero and display only an insignificant and numerically small trend with seawater pH ($R^2 = 0.33$, $P = 0.06$). Even though the observed deviation from zero could result from vital effects, e.g., an imprint from RubisCO on the internal isotope signal (McClelland et al., 2017), this value is yet perfectly in line with the notion that calcification does not fractionate strongly against its primary inorganic carbon source HCO_3^- (Rost et al., 2002; Sikes et al., 1980). The here observed trends towards higher $\Delta^{13}C_{PIC}$ and $\Delta^{13}C_{POC}$ values with increasing seawater pH have also been reported for another coastal coccolithophore, *O. neapolitana* (Liu et al., 2018), although those values were ~12‰ heavier (Fig. 5). Despite this offset, which cannot be explained with changes in carbon sources, the similar shifts of $\Delta^{13}C_{PIC}$ and $\Delta^{13}C_{POC}$ with seawater pH suggest that both coastal coccolithophore species increasingly utilize more CO_2 under more acidic conditions.

For *E. huxleyi,* the $\Delta^{13}C_{POC}$ and $\Delta^{13}C_{PIC}$ suggest major utilization of HCO_3^- for both, biomass buildup and calcification, which has been observed before (e.g., Kottmeier et al. (2016a, 2016b); Rokitta and Rost (2012)). The lack of pH-dependent trends, i.e., the comparably stable $\Delta^{13}C_{POC}$ and $\Delta^{13}C_{PIC}$ values indicate that changing carbon sources and changing leakage cancel each other out in *E. huxleyi* under the here applied growth conditions. There are fundamental uncertainties, however, regarding the fractionation behavior of the prime carbon fixing enzyme RubisCO in *E. huxleyi*, which hinder a more detailed discussion of the data (Boller et al., 2011).

Based on the $\Delta^{13}C_{POC}$, *C. leptoporus* seems to primarily use HCO_3^- in all pH scenarios, similar to what has been observed in *E. huxleyi*. Remarkably, both $\Delta^{13}C_{POC}$ and $\Delta^{13}C_{PIC}$ decrease when seawater pH increases, suggesting an apparently ceasing contribution of HCO_3^- to photosynthesis and calcification. This, however, contradicts our understanding of inorganic carbon transport and its pH/CO_2-dependent regulation (Reinfelder, 2011). Such patterns can thus only be explained by a significantly higher leakage over the plasmalemma under high pH that overcompensates the signal originating from the likely heavier carbon source under these conditions. Such a higher leakage can result from the steeper outward CO_2 gradient under high pH (i.e., low [CO_2]) and higher HCO_3^- pumping that result from the alleviation of H^+ inhibition (Kottmeier et al., 2016a).

4.3. Boron isotopic composition and its implication for calcification fluid pH

The boron isotope composition of the investigated coccolithophores show large variations in the experiments, spanning from 17‰ to 36‰ (Fig. 2(c)). *E. huxleyi* shows relatively constant values at about 25‰, which is in line

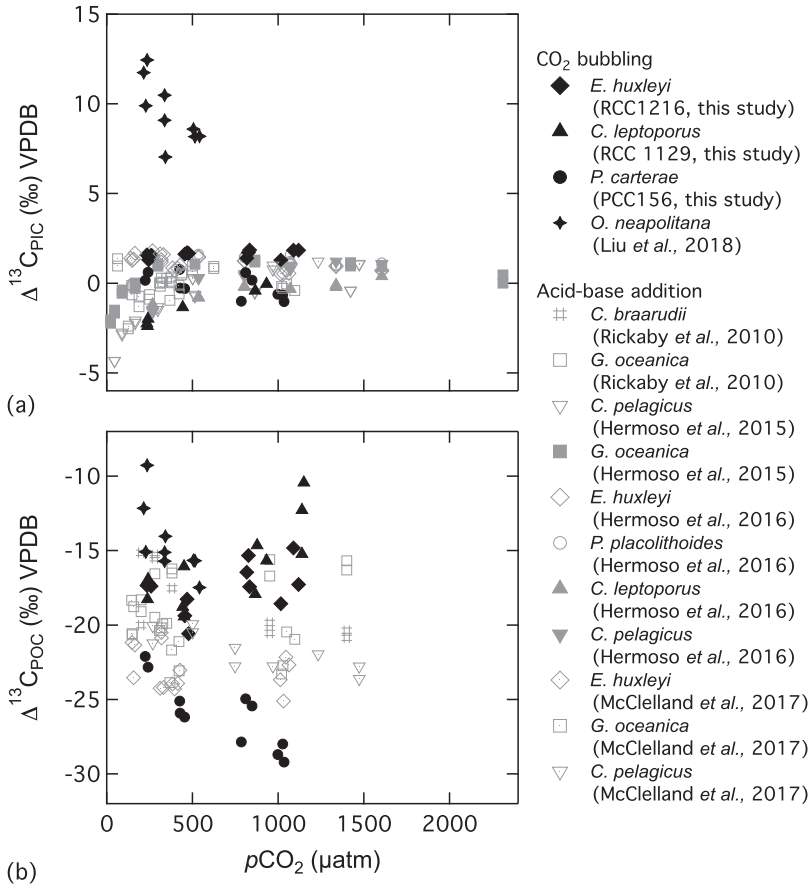

Fig. 5. Comparisons of stable carbon isotopes of the coccolithophore species examined in this study to other coccolithophore results from literature. (a) $\Delta^{13}C_{POC}$ and (b) $\Delta^{13}C_{PIC}$ values vs. atmospheric pCO_2 are plotted.

with reported $\delta^{11}B$ value ranging from 18‰ to 25‰ (Henehan, 2015). *C. leptoporus* exhibited $\delta^{11}B$ values between 19‰ to 35‰. For both species, no significant trend with decreasing seawater pH could be determined, which is consistent to previous findings in other coccolithophore species (Liu et al., 2018). *P. carterae* showed values from 17 to 36‰ that exhibit a significant correlation with seawater pH across the treatments. Absolute $\delta^{11}B$ values are different from those observed in *O. neapolitana* (Liu et al., 2018) due to the differences in the culture seawater $\delta^{11}B$ values. However, the range of $\delta^{11}B$ values derived in this study is comparable with these previous works, showing fractionation of about 15‰ to 22‰ with regard to the culture seawater $\delta^{11}B$ values (Henehan, 2015; Liu et al., 2018). Some of the $\delta^{11}B$ values of *C. leptoporus* and *P. carterae* determined here are about 5‰ to 10‰ higher than in those of *E. huxleyi* and *O. neapolitana*. These observed differences among species and deviations between studies have to be attributed to species-specific regulation of vesicle pH or, as an alternative hypothesis, they represent differences in uptake and transport of boron to the coccolith vesicle (see following sections).

Using the canonical systematics of the $\delta^{11}B$ proxy applications (Hemming and Hanson, 1992; Zeebe and Wolf-Gladrow, 2001) yields $\delta^{11}B$ inferred pH_{CF} values ranging between 7.8 and 9.5 for the investigated coccolithophores (Fig. 2(c)). These findings reflect that all three species increase pH_{CF} by at least 0.5 pH units, potentially up to ~ 1.5 pH units, above the surrounding pH_{SW} in almost all culture scenarios (Fig. 2(d)) to facilitate calcite precipitation. This underlines that those species are principally able to control their internal chemistry and overcome external pH levels to a considerable extent.

E. huxleyi and *C. leptoporus* experience little effect of pH_{SW} on their $\delta^{11}B$ signal (Fig. 2(c)). Apparently, they sustain relatively constant pH_{CF} of about 8.6 to 9.0 (Fig. 3(a)) to facilitate calcite precipitation (Fig. 1(e)) in all applied pH treatments, which is in good agreement with previous studies on *E. huxleyi* and *O. neapolitana* (Henehan, 2015; Liu et al., 2018). Hence, depending on external pH_{SW}, regulation of pH_{CF} is required to different extents, i.e., less effort under high pH. In contrast, *P. carterae* reveals a significant positive trend of increasing $\delta^{11}B$ with pH_{SW} (Fig. 2(c)), which implies that pH_{CF} (Fig. 3(a)) is kept at a constant pH offset of ~0.6 pH units with respect to the surrounding seawater (Fig. 2(d)). A possible explanation is that *P. carterae*'s calcification process is based on efficient vesicular Ca^{2+} (and potentially dissolved boron) delivery and is

strongly supported by the prominent coccolithosomes, which contain an organic polysaccharide matrix used for controlling calcite crystal growth (Holtz et al., 2013; Marsh and Dickinson, 1997). This molecular and subcellular control over coccolith formation may lower the need for strong pH elevation to achieve calcite precipitation conditions.

Additionally, we can evaluate the potential DIC_{CF} levels of the three coccolithophore species using both $\delta^{11}B$ and B/Ca for the calculation. Assuming a fixed minimum boron partition coefficient (K_D) of 0.0004 (Sanyal et al., 2000; Stoll et al., 2012), we derived that the DIC_{CF} in *E. huxleyi* is about 2–3 times higher than the DIC_{CF} in *C. leptoporus* and *P. carterae* (Fig. S9(b), Eq. (S1)). The calculated DIC_{CF} differences will be larger if we assume that the borate ion primarily competes with CO_3^{2-} instead of HCO_3^- when forming coccolith calcite (Fig. S9(c); see more detailed discussions on the potential control on the coccolith B/Ca in supplementary materials S2). Irrespective of how DIC_{CF} is calculated, for *E. huxleyi* and C. *leptoporus*, data suggest an interesting anticorrelation between achieved DIC_{CF} and pH_{CF}: *E. huxleyi*, a small cell, elevates DIC_{CF} 2–3 times higher than *C. leptoporus*, but achieves a lower pH_{CF}. The larger *C. leptoporus*, in turn, achieves a comparably low DIC_{CF}, but the highest pH_{CF} in our dataset. This way, the two species apparently create calcite-precipitating conditions in different ways. Given that *P. carterae*´s mode of calcification appears fundamentally different from the two aforementioned species, our data underline the high diversity in species-specific calcification mechanisms that were (re-)invented among the coccolithophores multiple times along their natural history (De Vargas et al., 2007).

4.4. Evaluation of assumptions on the $\delta^{11}B$ proxy

The application of the canonical $\delta^{11}B$ proxy for pH_{CF} in coccolithophores was based on several assumptions, most importantly, that only borate ions are incorporated into the coccolith calcite. Although recent NMR studies have revealed the complexity of boron incorporation into biogenic carbonates (Klochko et al., 2009; Noireaux et al., 2015; Rollion-Bard et al., 2011), the isotope signatures of studied carbonates suggest the variable proportions of trigonal B in the carbonates might be due to re-coordination of the tetrahedral $B(OH)_4^-$. An independent study with Near-Edge X-ray Absorption Fine Structure further provides some evidence that the trigonally coordinated BO_3 exists in calcite structure as a result of re-coordination and therefore strengthens the use of B as a pH proxy (Branson et al., 2015). However, it has also been suggested that both boric acid and borate ion incorporate into calcite (Cusack et al., 2015; Uchikawa et al., 2015). This can, at least for coralline red algae (Liu et al., 2020; Sutton et al., 2018), much better explain measured $\delta^{11}B$ values that are otherwise too high in some cases (>40‰) to be translated to a corresponding pH_{CF}. In contrast, in our study the lowest measured $\delta^{11}B$ value of ~17.5‰ from coccoliths is quite close to the lower limit of the theoretical seawater borate $\delta^{11}B$ curve calculated for the culture conditions. This would correspond to a maximum of ~10% of total boron being recruited from the boric acid pool for the process of coccolith formation.

Alternatively, we have calculated the pH_{CF}, as classically done for marine calcifiers, i.e., by assuming that the total boron isotopic composition of the calcification vesicle is in isotope equilibrium to the ambient seawater ($\delta^{11}B_{CF} = \delta^{11}B_{SW}$), and that only borate ion will be incorporated into coccolith calcite. We found that the pH_{CF} can vary across the pH treatments by as much as ~1.5 pH units (Fig. 3 (a)), sometimes reaching as high as ~9.5 in two of the species. It has been suggested that photosynthetic activities of organisms or the symbionts, as well as active proton regulation, can potentially raise the pH of the calcifying fluid to above 8.6 or even up to pH 9.3 in some organisms such as corals and coralline red alga (Ries, 2011; Short et al., 2015). Still, the absolute pH_{CF} values determined when applying this assumption are generally higher than reported observations of cytosolic or vesicle pH in *E. huxleyi* based on fluorescent dyes (Anning et al., 1996; Suffrian et al., 2011).

Based on observations in terrestrial plants and some animals (Dordas and Brown, 2000; Tanaka and Fujiwara, 2008), it has alternatively been proposed that boric acid is the primary dissolved boron source that crosses the cell membrane of coccolithophores by passive diffusion (Stoll et al., 2012). Taking this as an alternative hypothesis, the calculated pH_{CF} values are shifted down to mostly below pH 9.0 across the different treatments (Fig. 3(b)). Moreover, the range of the calculated pH_{CF} values would be about 0.2 units narrower and result in an increased sensitivity of pH_{CF} across the pH treatments for the three species (Fig. 3(c)). In this case, more of the determined pH_{CF} values would overlap with the independent determinations using pH sensitive dyes (Anning et al., 1996).

The partition coefficient of B to inorganic calcite has been estimated to be about 0.001 in an experiment with seeded crystal growth (Sanyal et al., 2000), but the solution chemistry was not fully documented and may therefore bear uncertainties. A lower estimation of K_D (0.0004–0.0005) has been proposed with the assumption that the seeded crystals were re-equilibrated with the experimental solution (Stoll et al., 2012). This lower estimation is similar to what has been found for foraminifera grown in seawater (Rollion-Bard and Erez, 2010). Thus, Stoll et al. (2012) assumed a fixed $K_D = 0.0005$ for coccolithophores, and modeled the expected B/Ca and $\delta^{11}B$ values of coccolith calcite under fixed or various pH_{CF} and vesicle DIC conditions (revised in Fig. 6). Here, we also compared our results to their model and found that only B/Ca ratios of *E. huxleyi* might fit in their "constant pH_{CF}" scenario (Fig. 6(a)). However, note that in the model, the $\delta^{11}B$ value of the calcification fluid will still change under different pH_{SW} due to the changes of $\delta^{11}B$ of boric acid transported to the cell.

In contrast to the model mentioned above, the $\delta^{11}B$ values we measured for *E. huxleyi* suggest a near identical $\delta^{11}B$ value of the calcification fluid, and thus contradict the assumption of diffusive boric acid uptake (Fig. 6(d, e)). Additionally, the higher B/Ca ratios measured for *C. leptoporus* and *P. carterae* (Fig. 4) suggest that K_D must be higher and/or variable to correctly describe calcite produc-

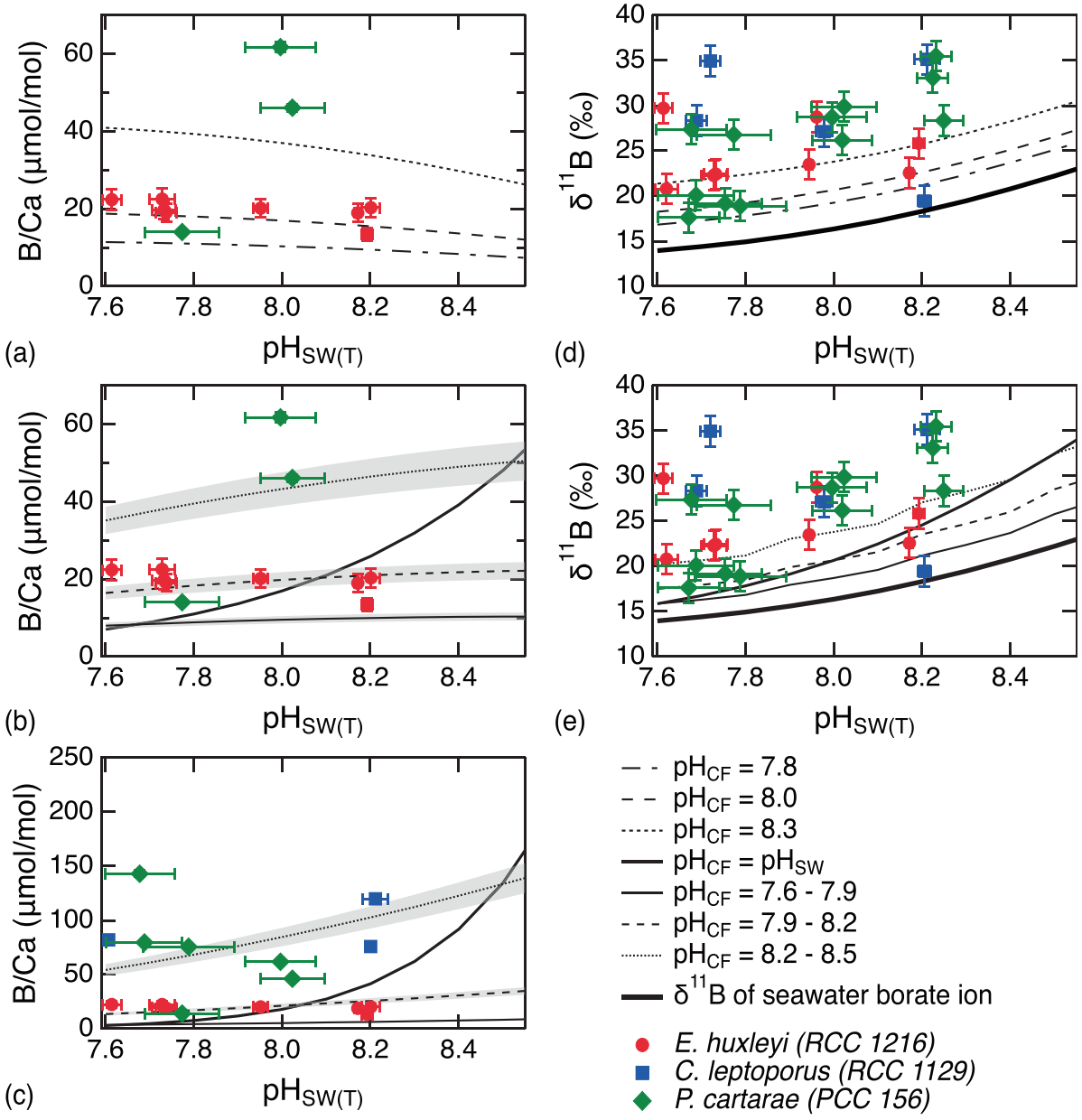

Fig. 6. Comparisons between the observed coccolithophore B/Ca and $\delta^{11}B$ and the model proposed by Stoll et al. (2012). Lines in (a) and (d) show predictions of coccolith B/Ca and $\delta^{11}B$ values for different pH_{CF} assuming pH is fixed in the coccolithophore calcification vesicle despite changing pH_{SW}. Lines in (b) and (e) show predictions of coccolith B/Ca and $\delta^{11}B$ values when vesicle pH is variable but DIC is fixed. Lines in (c) depict coccolith B/Ca and $\delta^{11}B$ values when both vesicle pH and DIC are variable. The shaded areas show the calculated B/Ca range of the pH interval. Data of present study are shown in solid symbols, with 1 RSD, 2SD, and 1 SD error bars in the B/Ca, $\delta^{11}B$, and pH_{SW} values, respectively. Note that the pH_{SW} values are all presented in total scale in this figure.

tion in these coccolithophore species. Although the $\delta^{11}B$-inferred pH_{CF} values in the second scenario (involving diffusive boric acid uptake) are lower and closer to what has been estimated from independent techniques (Anning et al., 1996), the above evaluations suggest that the assumptions of this scenario do not adequately describe the obtained data.

Although the actual boron uptake mechanism of coccolithophores is still unresolved, our boron isotope data provide more evidence that boric acid might not be the sole boron species that can pass through the cell membrane. Furthermore, our results reflect a general pH upregulation strategy among coccolithophore species under OA conditions. In addition, the experimental setting helps to evaluate the potential use of coccolith $\delta^{11}B$ as a paleo pH proxy. Based on our results, in only one of the four species examined, the coccolith $\delta^{11}B$ is sensitive to the changes of environmental seawater pH (Liu et al., 2018; this study)

suggesting coccolith calcite may not be an attractive target for paleo-ocean pH reconstruction. The systematic decline of $\delta^{11}B$ in *P. carterae* may indicate that this species could function as a potential archive for the use of paleo seawater pH reconstruction. However, that being said, the large variation within a treatment, the little amount of calcite as well as limited preservation in sediments likely hinders the applicability. Furthermore, an improvement of analytical precision for low boron concentration samples is required to better calibrate this potential proxy tool in the future.

5. CONCLUSION

Our results show highly variable signatures of incorporated boron and carbon isotopes, and B/Ca among three coccolithophore species across a wide range of seawater pH. The different isotopic compositions of organic and inorganic particulate carbon indicate different carbon utilization strategies among these species. Species-specific strategies are also evident from the boron isotopes and B/Ca data measured in the calcite. Our results highlight variability in the ability to regulate calcification fluid pH and to control carbonate chemistry in response to ocean acidification. Furthermore, our data demonstrates that the investigated species follow different mechanisms of calcite production and the associated carbon utilization. These findings are independent of underlying assumptions, and shed light on limitations of current models that aim to describe coccolithophores' boron uptake mechanisms, and the partition of boron species during coccolithophore calcification. Experiments like ours will add to our understanding of ion transport processes and how they may differ between species (Brownlee et al., 2020).

Declaration of Competing Interest

The authors declare that they have no known competing financial interests or personal relationships that could have appeared to influence the work reported in this paper.

ACKNOWLEDGEMENTS

We acknowledge Dr. Ina Benner and Dr. Chuan Ku for their helps in preparing additional coccolith materials for validation of coccolith cleaning protocols. This work was initially supported by an award to RAE under the the "Laboratoire d'Excellence" LabexMER (ANR-10-LABX-19), co-funded by a grant from the French government under the program "Investissements d'Avenir" and latterly a postdoctoral fellowship to YWL at Academia Sinica. This work was also supported by the Ministry of Science and Technology, Taiwan (MOST) to YWL. RAE also acknowledges support from National Science Foundation grant OCE-1437166 and the Pritzker Endowment to UCLA IoES.

AUTHOR CONTRIBUTIONS

RAE and YWL designed the research with input from SR and BR. YWL and SR performed the culturing. YWL performed the geochemical analyses and calculations. YWL drafted the manuscript with input from RAE, all authors contributed to the final manuscript.

DATA AVAILABILITY

All data needed to evaluate the conclusions in the paper are present in the paper and/or the Supplementary Materials. Additional data related to this paper may be requested from the authors.

APPENDIX A. SUPPLEMENTARY MATERIAL

Supplementary data to this article can be found online at https://doi.org/10.1016/j.gca.2021.09.025.

REFERENCES

Anning T., Nimer N., Merrett M. J. and Brownlee C. (1996) Costs and benefits of calcification in coccolithophorids. *J. Mar. Syst.* **9**, 45–56.

Blanco-Ameijeiras S., Lebrato M., Stoll H. M., Iglesias-Rodriguez M. D., Méndez-Vicente A., Sett S., Müller M. N., Oschlies A. and Schulz K. G. (2012) Removal of organic magnesium in coccolithophore calcite. *Geochim. Cosmochim. Acta* **89**, 226–239.

Boeckel B. and Baumann K.-H. (2004) Distribution of coccoliths in surface sediments of the south-eastern South Atlantic Ocean: ecology, preservation and carbonate contribution. *Mar. Micropaleontol.* **51**, 301–320.

Boller A. J., Thomas P. J., Cavanaugh C. M. and Scott K. M. (2011) Low stable carbon isotope fractionation by coccolithophore RubisCO. *Geochim. Cosmochim. Acta* **75**, 7200–7207.

Bolton C. T. and Stoll H. M. (2013) Late Miocene threshold response of marine algae to carbon dioxide limitation. *Nature* **500**, 558–562.

Branson O., Kaczmarek K., Redfern S. A. T., Misra S., Langer G., Tyliszczak T., Bijma J. and Elderfield H. (2015) The coordination and distribution of B in foraminiferal calcite. *Earth. Planet. Sci. Lett.* **416**, 67–72.

Brown P. H. and Hu H. (1993) Boron uptake in sunflower, squash and cultured tobacco cells: Studies with stable isotope and ICP-MS. *Plant Soil* **155**, 147–150.

Brownlee C., Langer G. and Wheeler G. L. (2020) Coccolithophore calcification: Changing paradigms in changing oceans. *Acta Biomater.*.

Casareto B. E., Niraula M. P., Fujimura H. and Suzuki Y. (2009) Effects of carbon dioxide on the coccolithophorid *Pleurochrysis carterae* in incubation experiments. *Aquat. Biol.* **7**, 59–70.

Cusack M., Kamenos N. A., Rollion-Bard C. and Tricot G. (2015) Red coralline algae assessed as marine pH proxies using 11B MAS NMR. *Sci. Rep.* **5**, 8175.

De Vargas C., Aubry M.-P., Probert I. A. N. and Young J. (2007) Origin and Evolution of Coccolithophores: From Coastal Hunters to Oceanic Farmers. In *Evolution of Primary Producers in the Sea* (ed. A. H. Knoll). Academic Press, Burlington, pp. 251–285.

Dickson Andrew G. (1981) An exact definition of total alkalinity and a procedure for the estimation of alkalinity and total inorganic carbon from titration data. *Deep Sea Res. Part A. Ocean. Res. Pap.* **28**(6), 609–623.

Dickson Andrew G. (1990) Standard potential of the reaction: $AgCl(s) + 1/2\ H_2(g) = Ag(s) + HCl(aq)$, and the standard

acidity constant of the ion HSO_4^- in synthetic sea water from 273.15 to 318.15 K. *J. Chem.Thermodyn.* **22**, 113–127.

Dickson A. G. and Millero F. J. (1987) A comparison of the equilibrium constants for the dissociation of carbonic acid in seawater media. *Deep-Sea Res.* **34**, 1733–1743.

Dickson A. G., Sabine C. L. and Christian J. R. (2007) *Guide to Best Practices for Ocean CO_2 Measurements*. North Pacific Marine Science Organization, Sidney.

Diez Fernández S., Encinar J. R., Sanz-Medel A., Isensee K. and Stoll H. M. (2015) Determination of low B/Ca ratios in carbonates using ICP-QQQ. *Geochem. Geophys. Geosyst.* **16**, 2005–2014.

Diner R. E., Benner I., Passow U., Komada T., Carpenter E. J. and Stillman J. H. (2015) Negative effects of ocean acidification on calcification vary within the coccolithophore genus *Calcidiscus*. *Mar. Biol.* **162**, 1287–1305.

Dittert N., Baumann K.-H., Bickert T., Henrich R., Huber R., Kinkel H. and Meggers H. (1999) Carbonate dissolution in the deep-sea: Methods, quantification and paleoceanographic application. In *Use of Proxies in Paleoceanography: Examples from the South Atlantic* (eds. G. Fischer and G. Wefer). Springer Berlin Heidelberg, Berlin, Heidelberg, pp. 255–284.

Dordas C. and Brown P. H. (2000) Permeability of boric acid across lipid bilayers and factors affecting it. *J. Membr. Biol.* **175**, 95–105.

Eichner M., Thoms S., Kranz S. A. and Rost B. (2015) Cellular inorganic carbon fluxes in Trichodesmium: A combined approach using measurements and modelling. *J. Exp. Bot.* **66**, 749–759.

Eikrem W., Medlin L. K., Henderiks J., Rokitta S., Rost B., Probert I., Throndsen J. and Edvardsen B. (2016) Haptophyta. In *Handbook of the Protists* (eds. J. M. Archibald, A. G. B. Simpson, C. H. Slamovits, L. Margulis, M. Melkonian, D. J. Chapman and J. O. Corliss). Springer International Publishing, Cham, pp. 1–61.

Fiorini S., Middelburg J. J. and Gattuso J.-P. (2011) Testing the effects of elevated pCO_2 on coccolithophores (*prymnesiophyceae*): Comparison between haploid and diploid life stages. *J. Phycol.* **47**, 1281–1291.

Geisen M., Billard C., Broerse A. T. C., Cros L., Probert I. A. N. and Young J. R. (2002) Life-cycle associations involving pairs of holococcolithophorid species: intraspecific variation or cryptic speciation? *Eur. J. Phycol.* **37**, 531–550.

Geisen M., Young J. R., Probert I., Sáez A. G., Baumann K.-H., Sprengel C., Bollmann J., Cros L., de Vargas C. and Medlin L. K. (2004) Species level variation in coccolithophores. In *Coccolithophores: From Molecular Processes to Global Impact* (eds. H. R. Thierstein and J. R. Young). Springer, Berlin Heidelberg, Berlin, Heidelberg, pp. 327–366.

Giordano M., Beardall J. and Raven J. A. (2005) CO_2 concentrating mechanisms in algae: Mechanisms, environmental modulation, and evolution. *Annu. Rev. Plant Biol.* **56**, 99–131.

Guillard R. R. L. and Ryther J. H. (1962) Studies of marine planktonic diatoms: I. *Cyclotella nana* Hustedt, and *Detonula confervacea* (cleve) Gran. *Can. J. Microbiol.* **8**, 229–239.

Hemming N. G. and Hanson G. N. (1992) Boron isotopic composition and concentration in modern marine carbonates. *Geochim. Cosmochim. Acta* **56**, 537–543.

Henehan M. J. (2015) *Ground-truthing the Boron-based Proxies*. Faculty of Natural and Environmental Sciences Ocean and Earth Sciences. University of Southampton, p. 348.

Hermoso M. (2015) Control of ambient pH on growth and stable isotopes in phytoplanktonic calcifying algae. *Paleoceanography* **30**, 2015PA002844.

Hermoso M., Chan I. Z. X., McClelland H. L. O., Heureux A. M. C. and Rickaby R. E. M. (2016) Vanishing coccolith vital effects with alleviated carbon limitation. *Biogeosciences* **13**, 301–312.

Hermoso M., Horner T. J., Minoletti F. and Rickaby R. E. M. (2014) Constraints on the vital effect in coccolithophore and dinoflagellate calcite by oxygen isotopic modification of seawater. *Geochim. Cosmochim. Acta* **141**, 612–627.

Hoins M., Eberlein T., Van de Waal D. B., Sluijs A., Reichart G.-J. and Rost B. (2016) CO_2-dependent carbon isotope fractionation in dinoflagellates relates to their inorganic carbon fluxes. *J. Exp. Mar. Biol. Ecol.* **481**, 9–14.

Hoins M., Van de Waal D. B., Eberlein T., Reichart G.-J., Rost B. and Sluijs A. (2015) Stable carbon isotope fractionation of organic cyst-forming dinoflagellates: Evaluating the potential for a CO_2 proxy. *Geochim. Cosmochim. Acta* **160**, 267–276.

Holtz L.-M., Langer G., Rokitta S. and Thoms S. (2013) Synthesis of nanostructured calcite particles in coccolithophores, unicellular algae. In *Green Biosynthesis of Nanoparticles: Mechanisms and Applications* (eds. M. Rai and C. Posten). CABI, Wallingford, UK.

Holtz L.-M., Wolf-Gladrow D. and Thoms S. (2017) Stable carbon isotope signals in particulate organic and inorganic carbon of coccolithophores – A numerical model study for *Emiliania huxleyi*. *J. Theor. Biol.* **420**, 117–127.

Hood M. A., Leemreize H., Scheffel A. and Faivre D. (2016) Lattice distortions in coccolith calcite crystals originate from occlusion of biomacromolecules. *J. Struct. Biol.* **196**, 147–154.

Hoppe C. J. M., Langer G., Rokitta S. D., Wolf-Gladrow D. A. and Rost B. (2012) Implications of observed inconsistencies in carbonate chemistry measurements for ocean acidification studies. *Biogeosciences* **9**, 2401–2405.

Hoppe C. J. M., Langer G. and Rost B. (2011) *Emiliania huxleyi* shows identical responses to elevated pCO_2 in TA and DIC manipulations. *J. Exp. Mar. Biol. Ecol.* **406**, 54–62.

Iglesias-Rodriguez M. D., Halloran P. R., Rickaby R. E. M., Hall I. R., Colmenero-Hidalgo E., Gittins J. R., Green D. R. H., Tyrrell T., Gibbs S. J., von Dassow P., Rehm E., Armbrust E. V. and Boessenkool K. P. (2008) Phytoplankton calcification in a high-CO_2 world. *Science* **320**, 336–340.

IPCC, 2013. Climate Change 2013: The Physical Science Basis. Working Group I Contribution to the IPCC 5th Assessment Report – Changes to the Underlying Scientific/Technical Assessment. Cambridge, United Kingdom and New York, NY, USA.

Klochko K., Cody G. D., Tossell J. A., Dera P. and Kaufman A. J. (2009) Re-evaluating boron speciation in biogenic calcite and aragonite using ^{11}B MAS NMR. *Geochim. Cosmochim. Acta* **73**, 1890–1900.

Klochko K., Kaufman A. J., Yao W., Byrne R. H. and Tossell J. A. (2006) Experimental measurement of boron isotope fractionation in seawater. *Earth. Planet. Sci. Lett.* **248**, 276–285.

Knappertsbusch M. (2000) Morphologic evolution of the Coccolithophorid *Calcidiscus leptoporus* from the early Miocene to recent. *J. Paleontol.* **74**, 712–730.

Knappertsbusch M., Cortes M. Y. and Thierstein H. R. (1997) Morphologic variability of the coccolithophorid *Calcidiscus leptoporus* in the plankton, surface sediments and from the Early Pleistocene. *Mar. Micropaleontol.* **30**, 293–317.

Kottmeier D., Rokitta S., Tortell P. and Rost B. (2014) Strong shift from HCO_3^- to CO_2 uptake in *Emiliania huxleyi* with acidification: new approach unravels acclimation versus short-term pH effects. *Photosynth. Res.* **121**, 265–275.

Kottmeier D. M., Rokitta S. D. and Rost B. (2016a) Acidification, not carbonation, is the major regulator of carbon fluxes in the coccolithophore *Emiliania huxleyi*. *New Phytol.* **211**, 126–137.

Kottmeier D. M., Rokitta S. D. and Rost B. (2016b) H^+-driven increase in CO_2 uptake and decrease in uptake explain coccolithophores' acclimation responses to ocean acidification. *Limnol. Oceanogr.* **61**, 2045–2057.

Langer G., Geisen M., Baumann K.-H., Klaes J. and Riebesell U. (2006) Species-specific responses of calcifying algae to changing seawater carbonate chemistry responses of calcifying algae. *Geochem. Geophys. Geosyst.* **7**.

Langer G., Nehrke G., Probert I., Ly J. and Ziveri P. (2009) Strain-specific responses of *Emiliania huxleyi* to changing seawater carbonate chemistry. *Biogeosciences* **6**, 2637–2646.

Liu Y.-W., Aciego S. M., Wanamaker A. D. and Sell B. K. (2013) A high-throughput system for boron microsublimation and isotope analysis by total evaporation thermal ionization mass spectrometry. *Rapid Commun. Mass Spectrom.* **27**, 1705–1714.

Lee Kitac, Kim Tae-Woo, Byrne Robert H., Millero Frank J., Feely Richard A. and Liu Yong-Min, et al. (2010) The universal ratio of boron to chlorinity for the North Pacific and North Atlantic oceans. *Geochim. Cosmochim. Acta* **74**(6), 1801–1811.

Liu Y.-W., Aciego S. M. and Wanamaker, Jr., A. D. (2015) Environmental controls on the boron and strontium isotopic composition of aragonite shell material of cultured *Arctica islandica*. *Biogeosciences* **12**, 3351–3368.

Liu Y.-W., Eagle R. A., Aciego S. M., Gilmore R. E. and Ries J. B. (2018) A coastal coccolithophore maintains pH homeostasis and switches carbon sources in response to ocean acidification. *Nat. Commun.* **9**, 2857.

Liu Y.-W., Sutton J. N., Ries J. B. and Eagle R. A. (2020) Regulation of calcification site pH is a polyphyletic but not always governing response to ocean acidification. *Sci. Adv.* **6**, eaax1314.

Marsh M. E. (2003) Regulation of $CaCO_3$ formation in coccolithophores. *Comp. Biochem. Physiol. B: Biochem. Mol. Biol.* **136**, 743–754.

Marsh M. E. and Dickinson D. P. (1997) Polyanion-mediated mineralization—mineralization in coccolithophore (*Pleurochrysis carterae*) variants which do not express PS2, the most abundant and acidic mineral-associated polyanion in wild-type cells. *Protoplasma* **199**, 9–17.

McClelland H. L. O., Bruggeman J., Hermoso M. and Rickaby R. E. M. (2017) The origin of carbon isotope vital effects in coccolith calcite. *Nat. Commun.* **8**, 14511.

McCulloch M. T., D'Olivo J. P., Falter J., Georgiou L., Holcomb M., Montagna P. and Trotter J. A. (2018) Boron isotopic systematics in Scleractinian corals and the role of pH up-regulation. In *Boron Isotopes: The Fifth Element* (eds. H. Marschall and G. Foster). Springer International Publishing, Cham, pp. 145–162.

Mehrbach C., Culberson C. H., Hawley J. E. and Pytkowicx R. M., et al. (1973) Measurement of the apparent dissociation constants of carbonic acid in seawater at atmospheric pressure. *Limnol. Ocean.* **18**(6), 897–907.

Meyer J. and Riebesell U. (2015) Reviews and Syntheses: Responses of coccolithophores to ocean acidification: a meta-analysis. *Biogeosciences* **12**, 1671–1682.

Moheimani N. R. and Borowitzka M. A. (2011) Increased CO_2 and the effect of pH on growth and calcification of *Pleurochrysis carterae* and *Emiliania huxleyi* (Haptophyta) in semicontinuous cultures. *Appl. Microbiol. Biotechnol.* **90**, 1399–1407.

Nir O., Vengosh A., Harkness J. S., Dwyer G. S. and Lahav O. (2015) Direct measurement of the boron isotope fractionation factor: Reducing the uncertainty in reconstructing ocean paleo-pH. *Earth. Planet. Sci. Lett.* **414**, 1–5.

Noireaux J., Mavromatis V., Gaillardet J., Schott J., Montouillout V., Louvat P., Rollion-Bard C. and Neuville D. R. (2015) Crystallographic control on the boron isotope paleo-pH proxy. *Earth. Planet. Sci. Lett.* **430**, 398–407.

Pierrot D. E., Lewis E. and Wallace D. W. R. (2006) MS Excel Program Developed for CO_2 System Calculations. ORNL/CDIAC-105a. *Carbon Dioxide Information Analysis Center, Oak Ridge National Laboratory, U.S. Department of Energy*. doi.10.3334/CDIAC/otg.CO2SYS_XLS_CDIAC105a.

Reinfelder J. R. (2011) Carbon concentrating mechanisms in eukaryotic marine phytoplankton. *Ann. Rev. Mar. Sci.* **3**, 291–315.

Rickaby R. E. M., Henderiks J. and Young J. N. (2010) Perturbing phytoplankton: response and isotopic fractionation with changing carbonate chemistry in two coccolithophore species. *Clim. Past* **6**, 771–785.

Riebesell U., Zondervan I., Rost B., Tortell P. D., Zeebe R. E. and Morel F. M. M. (2000) Reduced calcification of marine plankton in response to increased atmospheric CO_2. *Nature* **407**, 364–367.

Ries J. B. (2011) A physicochemical framework for interpreting the biological calcification response to CO_2-induced ocean acidification. *Geochim. Cosmochim. Acta* **75**, 4053–4064.

Rokitta S. D. and Rost B. (2012) Effects of CO_2 and their modulation by light in the life-cycle stages of the coccolithophore *Emiliania huxleyi*. *Limnol. Oceanogr.* **57**, 607–618.

Rollion-Bard C., Blamart D., Trebosc J., Tricot G., Mussi A. and Cuif J.-P. (2011) Boron isotopes as pH proxy: A new look at boron speciation in deep-sea corals using ^{11}B MAS NMR and EELS. *Geochim. Cosmochim. Acta* **75**, 1003–1012.

Rollion-Bard C. and Erez J. (2010) Intra-shell boron isotope ratios in the symbiont-bearing benthic foraminiferan *Amphistegina lobifera*: Implications for $\delta^{11}B$ vital effects and paleo-pH reconstructions. *Geochim. Cosmochim. Acta* **74**, 1530–1536.

Rost B. and Riebesell U. (2004) Coccolithophores and the biological pump: responses to environmental changes. In *Coccolithophores: From Molecular Processes to Global Impact* (eds. H. R. Thierstein and J. R. Young). Springer Berlin Heidelberg, Berlin, Heidelberg, pp. 99–125.

Rost B., Zondervan I. and Riebesell U. (2002) Light-dependent carbon isotope fractionation in the coccolithophorid *Emiliania huxleyi*. *Limnol. Oceanogr.* **47**, 120–128.

Rustad J. R., Bylaska E. J., Jackson V. E. and Dixon D. A. (2010) Calculation of boron-isotope fractionation between $B(OH)_3$(-aq) and $B(OH)_4$ (aq). *Geochim. Cosmochim. Acta* **74**, 2843–2850.

Sanyal A., Nugent M., Reeder R. J. and Bijma J. (2000) Seawater pH control on the boron isotopic composition of calcite: evidence from inorganic calcite precipitation experiments. *Geochim. Cosmochim. Acta* **64**, 1551–1555.

Seresinhe P. S. J. W. and Oertli J. J. (1991) Effects of boron on growth of tomato cell suspensions. *Physiol. Plant.* **81**, 31–36.

Short J. A., Pedersen O. and Kendrick G. A. (2015) Turf algal epiphytes metabolically induce local pH increase, with implications for underlying coralline algae under ocean acidification. *Estuar. Coast. Shelf Sci.* **164**, 463–470.

Sikes C. S., Roer R. D. and Wilbur K. M. (1980) Photosynthesis and coccolith formation: Inorganic carbon sources and net inorganic reaction of deposition1. *Limnol. Oceanogr.* **25**, 248–261.

Stoll M. H. C., Bakker K., Nobbe G. H. and Haese R. R. (2001) Continuous-Flow Analysis of Dissolved Inorganic Carbon Content in Seawater. *Analyt. Chem.* **73**(17), 4111–4116.

Stoll H., Langer G., Shimizu N. and Kanamaru K. (2012) B/Ca in coccoliths and relationship to calcification vesicle pH and dissolved inorganic carbon concentrations. *Geochim. Cosmochim. Acta* **80**, 143–157.

Suffrian K., Schulz K. G., Gutowska M. A., Riebesell U. and Bleich M. (2011) Cellular pH measurements in *Emiliania huxleyi* reveal pronounced membrane proton permeability. *New Phytol.* **190**, 595–608.

Sutton J. N., Liu Y. W., Ries J. B., Guillermic M., Ponzevera E. and Eagle R. A. (2018) $\delta^{11}B$ as monitor of calcification site pH in divergent marine calcifying organisms. *Biogeosciences* **15**, 1447–1467.

Takano J., Miwa K., Yuan L., von Wirén N. and Fujiwara T. (2005) Endocytosis and degradation of BOR1, a boron transporter of *Arabidopsis thaliana*, regulated by boron availability. *Proc. Natl. Acad. Sci. U. S. A.* **102**, 12276–12281.

Takano J., Noguchi K., Yasumori M., Kobayashi M., Gajdos Z., Miwa K., Hayashi H., Yoneyama T. and Fujiwara T. (2002) Arabidopsis boron transporter for xylem loading. *Nature* **420**, 337–340.

Tanaka M. and Fujiwara T. (2008) Physiological roles and transport mechanisms of boron: perspectives from plants. *Pflug. Arch. Eur. J. Physiol.* **456**, 671–677.

Uchikawa J., Penman D. E., Zachos J. C. and Zeebe R. E. (2015) Experimental evidence for kinetic effects on B/Ca in synthetic calcite: Implications for potential $B(OH)_4^-$ and $B(OH)_3$ incorporation. *Geochim. Cosmochim. Acta* **150**, 171–191.

van den Hoek C., Mann D. G. and Jahns H. M. (1995) *Algae: An Introduction to Phycology*. Cambridge University Press, pp. i-xiv, 1-623.

White M. M., Waller J. D., Lubelczyk L. C., Drapeau D. T., Bowler B. C., Balch W. M. and Fields D. M. (2018) Coccolith dissolution within copepod guts affects fecal pellet density and sinking rate. *Sci. Rep.* **8**, 9758.

Wilkes E. B. and Pearson A. (2019) A general model for carbon isotopes in red-lineage phytoplankton: Interplay between unidirectional processes and fractionation by RubisCO. *Geochim. Cosmochim. Acta* **265**, 163–181.

Zeebe R. E. and Wolf-Gladrow D. A. (2001) *CO_2 in Seawater: Equilibrium, Kinetics, Isotopes*. Elsevier Oceanography Series, Amsterdam.

Associate editor: Heather Stoll